Biochemistry

 Volume 29, Number 19 May 15, 1990

Perspectives in Biochemistry

Probing Protein Structure and Dynamics with Resonance Raman Spectroscopy: Cytochrome *c* Peroxidase and Hemoglobin†

Thomas G. Spiro,*,‡ Giulietta Smulevich,§ and Chang Su‡

Department of Chemistry, Princeton University, Princeton, New Jersey 08562, and Dipartimento di Chimica, Università di Firenze, Via G. Capponi 9, 50121 Firenze, Italy

Received October 31, 1989; Revised Manuscript Received December 14, 1989

Resonance Raman (RR) spectroscopy is increasingly being applied to biological molecules (Spiro, 1988). The technique involves laser scattering from a light-absorbing sample. The scattering spectrum contains peaks that report the frequencies of vibrational modes of the molecules being irradiated. Resonance occurs when the laser wavelength matches that of an electronic transition. Because of coupling between electronic and nuclear motions, certain vibrational modes are enhanced, those which mimic the distortion of the molecule in its resonant excited state (Spiro & Stein, 1977). For example, resonance with $\pi-\pi^*$ transitions enhances modes in which π bonds of the chromophore are stretched, while resonance with ligand–metal charge-transfer transitions in metal complexes enhances modes in which the metal–ligand bonds are stretched. This selectivity in the enhancement means that RR spectroscopy can be used as a probe for chromophoric sites in complex biological systems. Hemes, chlorophyll, flavins, the retinylidene cofactor of visual pigments and bacteriorhodopsin, and a variety of iron and copper metalloprotein sites are among the biological chromophores that have been examined by RR spectroscopy (Spiro, 1988). Recently the technique has been extended to aromatic protein residues (Hudson & Mayne, 1988) and to the purine and pyrimidine bases of nucleic acids (Tsubaki et al., 1988), thanks to the advent of practical UV laser sources (Ziegler & Hudson, 1983; Asher et al., 1983; Fodor et al., 1986; Jones et al., 1987).

Of course, selective enhancement also means a loss of information since many sites of molecular interest are nonchromophoric, although they can sometimes be labeled with extrinsic chromophores (Carey, 1988). Complete vibrational spectra can be obtained with nonresonance Raman spectroscopy, in which the laser wavelength is in a transparent region of the spectrum, or with infrared spectroscopy. The complete vibrational spectrum is very crowded for complex biological molecules, however, and it is difficult to associate a spectral feature with a particular site, although impressive results can be obtained with well-controlled difference spectra (Derguini et al., 1986; Chen et al., 1987). In those cases where the site of interest is chromophoric, RR spectra provide much more detailed structural information than nonresonance Raman or IR spectra.

The structural information in a vibrational spectrum is complementary to that produced by X-ray crystallography. Occasionally an error in a crystal structure determination can be detected by vibrational spectroscopy, as in the case of the 3-Fe center of *Azotobacter vinelandii* ferredoxin I, for which the original report of a hexagonal Fe_3S_3 ring (Ghosh et al., 1982) was shown to be incompatible with the RR spectrum (Johnson et al., 1983) [other spectroscopic probes also threw doubt on this structure (George et al., 1984)]; the structure was later redetermined (Stout et al., 1988; Stout, 1988) and shown to be a Fe_4S_4 cube with a missing corner, as had earlier been proposed on the basis of chemical evidence (Beinert & Thomson, 1983). Only X-ray crystallography, or, for relatively small macromolecules, 2-D NMR spectroscopy, can produce the full three-dimensional arrangement of all the atoms, however. What vibrational spectroscopy can provide is a monitor of the strengths of bonds and the conformations of molecular fragments, as they interact with their environments. The vibrational frequencies are highly sensitive to these molecular parameters, which are at the heart of biological activity.

In this review the kinds of information available from RR spectroscopy are illustrated with new results on two heme proteins, cytochrome *c* peroxidase (CCP) and hemoglobin (Hb). CCP is a peroxide-utilizing enzyme (Yonetani, 1976), whose chemistry is determined by interactions between the heme prosthetic group and the protein residues lining the heme pocket. These interactions are many and subtle, and they can be varied systematically by site-directed mutagenesis of cloned protein (Mauro et al., 1989; Goodin et al., 1986). RR spec-

† This work was supported by NIH Grant GM33576.
‡ Princeton University.
§ Università di Firenze.

0006-2960/90/0429-4497$02.50/0

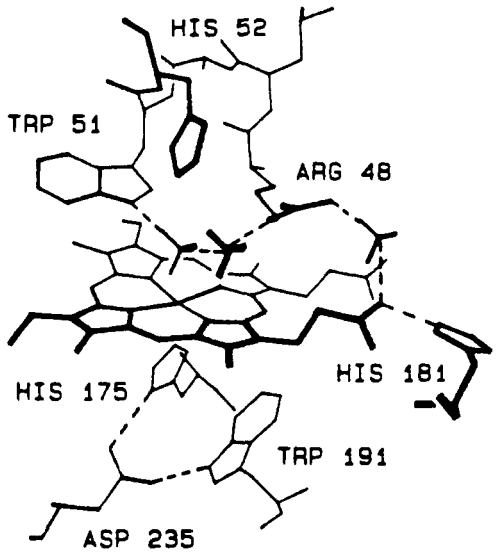

FIGURE 1: View of the heme group in bakers' yeast CCP and the surrounding residues that provide important interactions. H-Bonds are indicated by dotted lines. The tetrahedra represent water molecules localized on the distal side of the heme. From Finzel et al. (1986).

troscopy has proven to be a useful monitor of these interactions. Hb is limited to the simple function of binding O_2, but it does so cooperatively, via an allosteric transition. Because of intensive studies in many laboratories, Hb has become the paradigmatic molecule with which to understand allostery (Perutz, 1975; Perutz et al., 1987). A promising approach is to investigate the kinetic steps in the quaternary transition between the R (relaxed) and T (tense) state of the molecule. RR spectroscopy, applied in a time-resolved mode, has provided structural information about the intermediates in this process.

The reader is referred to recent reviews on the detailed interpretation of metalloporphyrin RR spectra (Spiro & Li, 1988) and of the RR signals associated with endogenous (Kitagawa, 1988; Champion, 1988) and exogenous (Kerr & Yu, 1988) heme protein ligands, as well as of protein aromatic residues (Hudson & Mayne, 1988). This information is relevant to the ensuing discussion, but much of it has been omitted in the interest of brevity and clarity.

Cytochrome *c* Peroxidase: A Balance of Protein–Heme Forces

Proximal Imidazole/Imidazolate. Figure 1 shows the disposition of residues in the heme pocket of CCP, as determined from the crystal structure of protein from bakers' yeast (Finzel et al., 1986). A very similar structure is found for the engineered protein CCP(MI), expressed in *Escherichia coli* (Wang et al., 1989). In common with the globins, the heme Fe atom in CCP is bound to the protein through an N atom of an imidazole side chain (His-175), but the H-bond status of the other imidazole N atom is distinctive. In the globins this proton interacts with a (neutral) peptide carbonyl group of the backbone, whereas in CCP the interaction is with the anionic carboxylate side chain of Asp-235. The proximal H-bond is much stronger in CCP, and gives the ligand substantial imidazolate character, thereby strengthening its donor interaction with Fe. This interaction can be monitored directly via the frequency of the Fe–N(His) stretching vibration, which gives rise to a prominent band near 200 cm^{-1} in RR spectra of Fe(II) heme proteins, identifiable via its characteristic ^{54}Fe shift. In myoglobin (Mb) this band is at 220 cm^{-1} (Kitagawa et al., 1979; Argade et al., 1984), whereas in CCP (Hashimoto et al., 1986; Smulevich et al., 1986; Dasgupta et al., 1989) and also in horseradish peroxidase (HRP) and other plant peroxidases (Teraoka & Kitagawa, 1981; Teraoka et al., 1983) it is near 240 cm^{-1}.

In a model study with 2-methylimidazole (2-MeImH) bound to Fe(II) protoheme, the Fe–2-MeImH frequency was found to be 205 cm^{-1} in benzene but 220 cm^{-1} in water and 239 cm^{-1} when the imidazole proton was removed with a strong base in dimethylformamide (Stein et al., 1980). These are large shifts and reflect considerable sensitivity of the Fe–imidazole bond strength to the status of the proton on the bound imidazole. When this proton is removed, leaving an anionic imidazolate ligand, the bond strength increases by about one-third, judging from the 35% increase in force constant which is implied by the frequency shift from 205 cm^{-1} in benzene to 239 cm^{-1} in strong base/dimethylformamide. The 220-cm^{-1} frequency observed in water implies that H-bond donation to water molecules produces about half as much increase in the bond strength as does deprotonation. In comparing these values with the frequencies observed in protein, about 10 cm^{-1} should be added to the former in order to account for the steric encumbrance of the 2-methyl group in the model complexes (M. Mitchell and T. G. Spiro, unpublished results); [this steric encumbrance serves to inhibit bis-imidazole adduct formation (Collman & Reed, 1973)]. Thus, the 220-cm^{-1} frequency of Mb indicates that the proximal H-bond to the backbone carbonyl group is weaker than an H-bond between Fe-bound imidazole and water, while the 240-cm^{-1} frequency of CCP indicates that the H-bond to the Asp-235 carboxylate is stronger.

The proximal H-bond may play several roles in peroxidase activity. The increased imidazolate character certainly helps to lower the Fe(III/II) reduction potential, −194 vs +50 mV for Mb (Cassatt et al., 1975), by stabilizing the Fe(III) form, the form that reacts with peroxide. By the same token, imidazolate stabilizes the Fe^{IV}=O intermediate (Edwards et al., 1987) resulting from heterolytic cleavage of the bound peroxide. Finally, the rate of release of the product, H_2O, of the electron-transfer reaction, is increased because of lowered H_2O affinity in the resting enzyme; both electronic [lowered Fe(III) charge density due to the partially anionic character of the ligand] and steric (anchoring of the Fe ion below the heme plane by the proximal H-bond) factors may be involved in the stabilization of 5-coordinate Fe(III) heme in CCP (see below).

Dramatic confirmation of the importance of the His-175–Asp-235 H-bond to the Fe–N(His) bond strength was obtained via the Asn-235 mutant, whose RR spectrum (Smulevich et al., 1988a) is compared with that of CCP(MI) in Figure 2. The broad ~240-cm^{-1} Fe–N(His) band of the latter is missing for the mutant and is replaced by a narrow band at 205 cm^{-1}, which is tentatively assigned to Fe–N(His) stretching. This is a much lower frequency than that of Mb and implies that the H-bond to the Asn-235 side chain is extremely weak. Interestingly, the crystal structure of the Asn-235 mutant shows the indole ring of Trp-191, which is also H-bonded to the Asp-235 carboxylate side chain in native CCP, to be flipped over and H-bonded to the carbonyl group of Leu-177 (Mauro et al., 1989). Thus, the carboxylate interactions with both of the H-bond donors, His-175 and Trp-191, are greatly attenuated upon replacement with the neutral carboxamide side chain. Trp-191 has been shown to be the residue giving rise to a unique axial EPR radical signal in the two-electron-oxidized ES intermediate arising from the reaction of CCP with hydroperoxides (Sivaraja et al., 1989). This signal is lost, and activity is greatly reduced, when Trp-191 is replaced by Phe. Thus another role for Asp-235 may be to anchor Trp-191 in

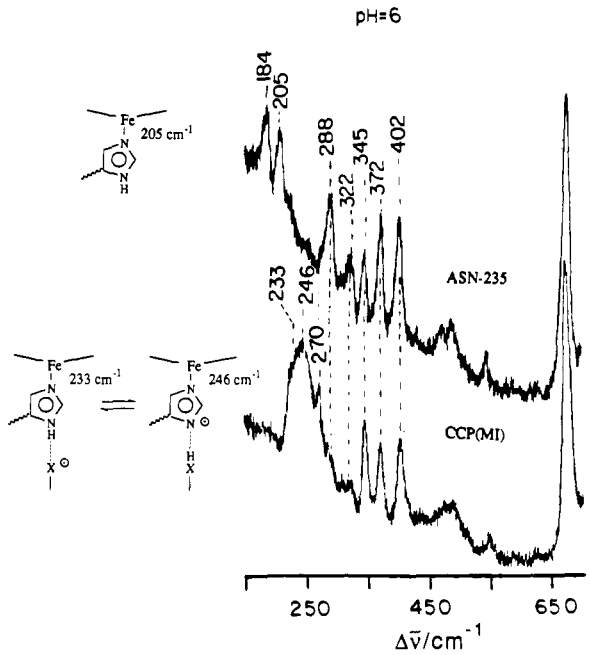

FIGURE 2: Low-frequency RR spectra of Fe(II) forms of CCP(MI) and of the Asn-235 mutant, obtained with 441.6-nm excitation [experimental details in Smulevich et al. (1988a)]. The broad ~240-cm^{-1} Fe–N(His) stretching band of CCP(MI) has 233- and 246-cm^{-1} components, which are suggested to arise from a double-well potential in which the proton can reside on the proximal imidazole (233 cm^{-1}) or on the interacting carboxylate group of Asp-235 (246 cm^{-1}). Replacement of the carboxylate group by the carboxamide side chain of Asn eliminates the 240-cm^{-1} band and replaces it with one at 205 cm^{-1}, indicating that the proximal H-bond is very weak.

an orientation close to (and parallel with; see Figure 1) the proximal heme ligand, thereby facilitating electron transfer.

The breadth of the Fe–N(His) band is of interest. There are actually two components, at 233 and 246 cm^{-1}. Their relative intensities are altered at high pH (Hashimoto et al., 1986), leading to an apparent downshift in the entire band (Dasgupta et al., 1989), and also when various side chains are altered in the heme pocket (Smulevich et al., 1988). This behavior implies two forms of the proximal ligand, the populations being sensitive to the disposition of other side chains in the pocket. The 246-cm^{-1} frequency is so high that complete deprotonation is indicated, while the 233 cm^{-1} frequency is consistent with a fairly strong H-bond. It was therefore suggested (Smulevich et al., 1988) that the two forms arise from the proton being in a double-well potential. It resides on the imidazole in one minimum, corresponding to the 233-cm^{-1} frequency, and on the Asp-235 carboxylate in the other, corresponding to the 244-cm^{-1} frequency. The comparable intensities of the two components suggest that the two minima are nearly isoenergetic. At first sight it is surprising that the proton should be nearly equally shared by the imidazolate and carboxylate anions, given their vastly different pK_a's, ~14 and ~4.5, in aqueous solution. But the proximal linkage is isolated from solvating water molecules, and the imidazolate basicity is diminished by coordination to the Fe(II). The latter effect should be even more pronounced for higher Fe oxidation states, which should shift the balance further toward imidazolate. Indeed, NMR data on the CN^- adduct of Fe(III) HRP show that the proximal imidazole proton is transferred to another protein residue (La Mar & de Ropp, 1979).

Distal H-Bonding to the CO Adduct. When RR and IR spectra are examined for CO adducts of CCP variants, three vibrational patterns emerge, as exemplified by the spectra of CCP(MI) and its Phe-51 mutant (Smulevich et al., 1988b),

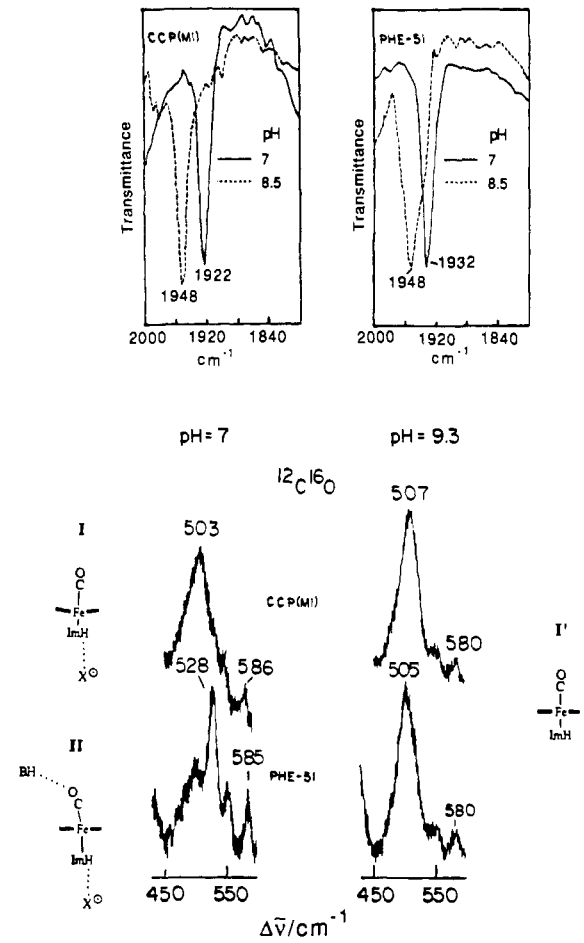

FIGURE 3: RR bands associated with Fe–CO stretching (500–530 cm^{-1}) and Fe–C–O bending (585 cm^{-1}) and the IR band due to C–O stretching (~1920–1960 cm^{-1}) for CO adducts of CCP(MI) and the Phe-51 mutant at neutral and high pH [experimental details in Smulevich et al. (1988b)]. These adducts illustrate the three forms, I and II (neutral and low pH) and I′ (high pH), encountered among CCP variants. The inferred bonding arrangements (see text) are shown in the diagram.

shown in Figure 3. These patterns are interpreted as arising from different structures, labeled form I, II, and I′, respectively. Form I′ is exhibited by all CCP variants at alkaline pH and is believed to reflect a standard CO adduct with an ordinary imidazole ligand. Forms I and II are formed at acid pH and are favored by different variants. Form I is attributed to a CO adduct with a ligand having substantial imidazolate character whereas in form II the CO adduct receives a distal H-bond to its O atom while the Fe–imidazole bond is concomitantly weakened.

These structural inferences are based on the correlation of the frequencies of the Fe–CO (~500 cm^{-1}) and C–O (~1950 cm^{-1}) stretching vibrations, ν_{Fe-CO} and ν_{C-O}, seen in Figure 4. For a large number of CO adducts of Fe(II) porphyrins having imidazole ligands, the data follow the straight line (Kerr & Yu, 1988; Uno et al., 1987; Li & Spiro, 1988b) shown in Figure 4. Its negative slope reflects the role in Fe–CO bonding of the back-donation of Fe electrons in the filled d_π orbitals to the empty π^* orbitals of the CO ligand. As back-donation increases, so does the Fe–CO bond strength, whereas the C–O bond strength decreases. Likewise, the stretching frequencies change in an inverse manner. Influences that increase back-donation move the data points upward along the line in Figure 4. The polarity of the CO environment is an important factor, since back-bonding increases the negative charge on the O atom and the developing charge is stabilized by interactions

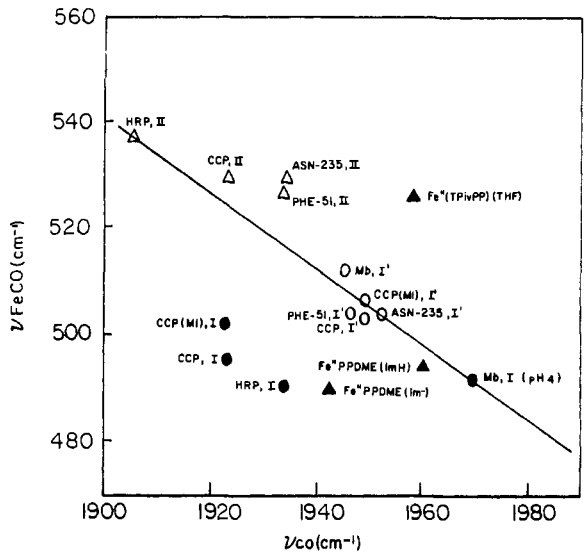

FIGURE 4: Correlation of ν_{Fe-CO} with ν_{C-O} for heme–CO adducts. The straight line ($\nu_{Fe-CO} = 1965-0.75\nu_{C-O}$ cm^{-1}) fits those adducts having an axial imidazole ligand with a weak or absent H-bond (Li & Spiro, 1988b). Stronger σ donor ligands produce negative deviations from the lines while weaker donors produce positive deviations. Symbols: (▲) model compounds from protoporphyrin dimethyl ester (PPDME) or "picket fence" porphyrin (TPivPP) with imidazole (ImH), imidazolate (Im), and tetrahydrofuran (THF) ligands; (●) form I, (○) form I′, and (△) form II CO adducts of the indicated protein.

with polar solvent molecules or distal protein residues. A major influence of this kind is H-bonding from a distal residue, which enhances back-donation by compensating the negative charge built up on the O atom of the CO. Distal H-bonding has been demonstrated for form II CO adducts of HRP (Smith et al., 1983) and CCP (Satterlee & Erman, 1984) via ν_{C-O} shifts in D_2O. This interaction is the reason that the data points for form II adducts lie at the high end of the plot in Figure 4. H-Bonding is not present for the alkaline form I′ adducts, which lie much lower on the line, near the point for Mb; the CO adduct is known not to be H-bonded in Mb (Kuriyan et al., 1986).

Data points fall significantly above or below the line in Figure 4 when the axial ligand is a weaker or stronger σ donor than imidazole (Li & Spiro, 1988b). As the σ donation increases, so does the electron density on the Fe. Consequently, back-donation increases, and ν_{C-O} is lowered, but the expected increase in ν_{Fe-CO} is offset by competition between CO and the donor ligand for the Fe σ orbital (d_{z^2}). This competition weakens the Fe–CO bond. For example, negative deviations are shown by CO adducts of cytochrome P-450 enzymes (Uno et al., 1987), which have strongly donating thiolate ligands. Likewise, deprotonation of imidazole bound to a heme–CO adduct (Figure 4) produces a negative deviation, since imidazolate is a stronger σ donor. The negative deviations of the form I adducts are attributed to the imidazolate character of the proximal ligand, as demonstrated by the RR spectroscopy on the Fe(II) protein. Since, however, the data points for the form II and form I′ adducts fall close to the line in Figure 4, it may be inferred that imidazolate character is no longer pronounced in these forms. Either the proximal H-bond is significantly weakened, or the Fe–N(His) bond is actually stretched in the protein. In fact, this bond does appear to be stretched in the recently determined crystal structure of the CO adduct of bakers' yeast CCP (Edwards & Poulos, 1989).

The Fe–N(His) bond weakening in the form II adducts suggests that the steric requirements for distal and proximal H-bonding are not mutually compatible. This structural hypothesis is consistent with the observations that CCP(MI) favors form I, while the Asn-235 mutant, which lacks the proximal H-bond, favors form II (Smulevich et al., 1988). A mixture of forms I and II is obtained in the Phe-191 mutant; apparently, the loss of the Trp-191–Asp-235 H-bond, which anchors the His-175–Asp-235 H-bond, allows the distal CO H-bond to form in a fraction of the molecules. Likewise, a mixture is seen for the His-181 mutant (Smulevich et al., 1989b), probably reflecting the increased mobility of the six-residue loop connecting the proximal His-175 with His-181, which is H-bonded to a heme propionate group (Figure 1). Residue replacements on the distal side also alter the form I/II energetics. Thus, the Phe-51 mutant favors form II (Figure 3); this may result from a small displacement of the entire distal (B) helix seen in the crystal structure (Wang et al., 1989). On the other hand, replacement of Arg-48 with Leu or Lys does not favor form II. Crystal structures are not yet available for these mutants, but it seems likely that the substitutions influence the position of His-52.

Interestingly, a mixture of forms I and II is also seen for bakers' yeast CCP (Smulevich et al., 1986) but not for CCP(MI). The structures of these two proteins are very similar but not identical. The main difference is a slight (0.5 Å) shift of the His-52 residue relative to the heme, resulting from the altered helix interactions associated with the Thr-53 → Ile substitution in CCP(MI) (Wang et al., 1989). The crystal structure of the CO adduct of bakers' yeast CCP shows that His-52 does H-bond to the CO, so this shift could well account for the stability of form II. Actually, the form II stability was found to be marginal (Smulevich et al., 1986) since it was the dominant form in bakers' yeast CCP only when the protein was exposed to CO at 1-atm pressure. At lower pressure, form I was favored. This behavior was interpreted to mean that binding of a second molecule of CO somewhere in the protein is required to tip the energy balance toward form II. Similar behavior was found for HRP (Evangelista-Kirkup et al., 1986).

While the weakening of the proximal linkage in the form II adducts can be understood in terms of the distal H-bond requirements, a more delocalized protein rearrangement is required to explain the proximal weakening in the alkaline form I′ adducts, for which no significant distal interaction is evident. It may be significant that the acid/alkaline transition involves a two-proton titration (Iizuka et al., 1985; Miller et al., 1990). One proton is probably removed from His-52, accounting for the loss of the distal H-bond, and the other may come from His-181. The latter deprotonation might trigger a proximal alteration via the His-181–His-175 loop.

In addition to ν_{Fe-CO} and ν_{C-O}, the Fe–C–O bending mode, δ_{Fe-C-O}, which is absent in RR spectra of unconstrained CO adducts, in which the CO assumes its normal upright position, becomes observable in some heme proteins, including Mb (Tsubaki et al., 1982), as well as for Fe porphyrins having a synthetic "strap" (Yu et al., 1983) or "cap" (G. Ray, X.-Y. Li, J. L. Sessler, and T. G. Spiro, unpublished results) that hinders upright binding sterically. The MbCO crystal structure (Kuriyan et al., 1986) shows that the distal His residue provides steric hindrance to upright binding, and the CO is off axis. Whether the FeCO unit is bent or tilted is not readily determined because of disorder in the crystal, and this question has been a matter of some debate. On the basis of force constant considerations, a concerted distortion model has been proposed, in which the FeCO is mostly tilted, but slightly bent, and the off-axis displacement is also accommodated by a degree of porphyrin buckling (Li & Spiro, 1988b). This

model was strikingly borne out by the subsequent high-resolution crystal structure of the CO adduct of a sterically hindered "capped" porphyrin, which showed just these features (Kim et al., 1989). The δ_{Fe-C-O} mode gains RR activity in these constrained systems because the loss of axial symmetry provides an enhancement mechanism which is otherwise absent (Li & Spiro, 1988b). Thus the RR intensity of this mode can be taken as an indication of off-axis binding, although it is possible that other symmetry-lowering perturbations, e.g., asymmetric electrostatic fields in the heme pocket, may play a role. The mode is fairly prominent in form II CCP adducts (Figure 3), consistent with the distal H-bond being off-axis and resulting in a tilted Fe–C–O unit (Edwards & Poulos, 1989). This potential for off-axis H-bonding to the diatomic ligand is undoubtedly relevant to the mechanism of O–O bond heterolysis in the peroxide reaction (Poulos, 1988).

The weakness of the δ_{Fe-C-O} mode in the form I and form I′ adducts suggests minimal off-axis influence in these forms. Thus the residues on the distal side of the heme offer little or no steric hindrance to upright binding of CO, consistent with the open pocket seen on the distal side in the crystal structure (Figure 1). CCP–CO offers an interesting structural contrast with MbCO. The data points of the alkaline forms (I′) of both proteins fall near one another on the line in Figure 4, indicating similar electronic states, but MbCO has a prominent δ_{Fe-C-O} RR band, consistent with the known off-axis geometry. When the distal His residue of Hb, His-64, is protonated, the δ_{FeCO} mode is deactivated, indicating upright binding of the CO (Ramsden & Spiro, 1989). Moreover, the low-pH Mb I data point in Figure 4 moves down the line. This indication of decreased back-bonding probably results from movement of His-64 out of the distal pocket, leaving only nonpolar residues near the CO. [The frequencies are close to those of an imidazole–heme–CO adduct in benzene (Ramsden & Spiro, 1989).] Protonation of the distal histidine does not lead to H-bond formation with the CO, as it does in the CCP form II adduct; if it did, the data point would move up the line in Figure 4. Moreover, the pK_a is strongly depressed, to ~4.2, in MbCO (Ramsden & Spiro, 1989), whereas it is quite normal, ~7.5, in CCP-CO. The difference must lie in the different distal stereochemistry in the two proteins. The distal His residue crowds the CO in Mb and is poorly disposed for H-bonding upon protonation. Consequently, protonation of the distal His is not stabilized by interaction with the CO. In CCP-CO the distal His-52 is further from the heme and can H-bond to the O atom of the CO (Edwards & Poulos, 1989).

Fe Ligation State in Native Protein: A Balancing Act. Subtle interactions between the heme and the residues lining the pocket also influence the coordination state of CCP in the absence of added ligands. The coordination state is conveniently monitored via the frequencies of porphyrin skeletal modes in the 1450–1650-cm^{-1} region of the RR spectrum (Li & Spiro, 1988a). These frequencies vary inversely with the porphyrin core size (Parthasarathi et al., 1987), since they involve stretching of the bonds to the methine bridges, where core size changes are largely accommodated. The core size depends on the ligation state because of the electronic properties of the Fe ions (Li & Spiro, 1988a). When two strong-field ligands are bound to the heme, the Fe valence electrons are maximally paired (low spin) in the nonbonding d_π orbitals, and the bonds to Fe are short, ~2.00 Å. When two weak-field ligands are bound, the Fe electrons occupy the antibonding d_σ orbitals, in order to minimize interelectronic repulsion, and are maximally unpaired (high spin). The metal–ligand bonds are thereby lengthened, and the core size increases, to a radius of ~2.04 Å for Fe^{III} and ~2.06 Å for Fe^{II}. Alternatively, the high-spin heme can be 5-coordinate, in which case the Fe atom moves out of the plane toward the fifth ligand and the core relaxes to an intermediate size. When imidazole is the fifth ligand, as in the globins and the peroxidases, the Fe(II) state is 5-coordinate (5-c) and high spin, unless there is a strong-field sixth ligand, either exogenous or endogenous, which produces a low-spin 6-coordinate (6-c) complex. In the Fe^{III} state the heme can also be 5-c, but it can bind weak-field (e.g., F^-) as well as strong-field ligands. When H_2O or OH^- is bound, the resulting complexes are typically mixed spin, and the spin population is temperature dependent, since these ligands, in combination with imidazole, produce Fe^{III} ligand fields that are close to the spin crossover.

The best core-size marker mode is ν_3, near 1500 cm^{-1}, a spectral region free of overlaps from other modes. ν_3 has characteristic frequencies for 5- and 6-c, high- and low-spin Fe(II) and Fe(III) hemes. For Fe(II) CCP its frequency is characteristic of 5-coordination (Smulevich et al., 1986), as expected since the heme is high spin. At alkaline pH the absorption spectrum shows a clear-cut transition to a low-spin product (Iizuka et al., 1985; Miller et al., 1990), but in several studies the RR spectrum was reported (Hashimoto et al., 1986; Dasgupta et al., 1989; Smulevich et al., 1988) to show a high-spin heme. This discrepancy has recently been traced to a reversible photolysis of the low-spin product by the Raman laser (Smulevich et al., 1989c). The alkaline conversion to the low-spin state requires binding of an endogenous ligand, which is evidently photolabile. The only plausible endogenous ligand is the distal His-52 side chain [an alkaline low-spin complex is still found if Trp-51 is replaced by Phe or Arg-48 is replaced by Leu (Smulevich et al., 1988)], but the resulting bis-imidazole complex would not be expected to be photolabile, on the precedent of model complexes or other heme proteins. Recent picosecond transient absorption measurements have shown, however, that the apparent photostability of the Fe–imidazole bond is due to rapid and efficient recombination of the imidazole following photolysis (Jogenward et al., 1988). Thus, the appearance of a high-spin heme during laser irradiation of alkaline Fe(II) CCP can be explained if the recombination of photodissociated His-52 is less efficient than a normal imidazole. The His-52 is 5.8 Å from the Fe in the crystal structure of Fe(III) protein (Finzel et al., 1986), and its binding to Fe(II) at alkaline pH must involve a substantial reorganization of the protein structure. If the energy required for this reorganization induces a strain in the Fe–His-52 bond, then the inefficient recombination could be readily explained. Such a strain would also provide an explanation for the finding that the rate of CO binding to Fe(II) CCP is unusually fast in the alkaline form, despite its being 6-c (Miller et al., 1990).

In the Fe(III) form of CCP the heme is likewise low spin at alkaline pH, as illustrated in Figure 5 (bottom). The sixth ligand may again be His-52, but it is more likely to be OH^-, which has a much higher affinity for Fe(III) than for Fe(II). OH^- is definitely bound to alkaline Fe(III) HRP as shown by the identification of an Fe–OH stretching band in the RR spectrum (Sitter et al., 1988). At acid pH the Fe(III) heme is high spin and 5-c, in both CCP and HRP. The CCP crystal structure shows a water molecule (Figure 1), W595, above the Fe but far enough away, 2.4 Å [2.7 Å in CCP(MI)], to preclude coordination. At low temperatures both EPR (Yonetani & Anni, 1987) and RR (Smulevich et al., 1989b) spectroscopies show conversion to a low-spin heme, suggesting that the factors inhibiting the binding of W595 to the Fe are overcome when thermal fluctuations are damped out.

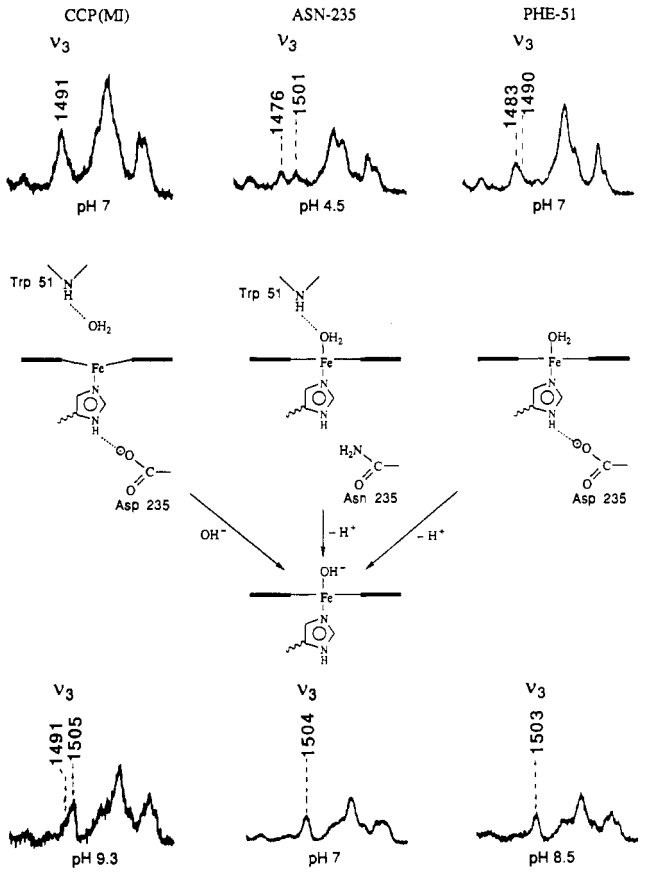

FIGURE 5: High-frequency region of the RR spectra (413.1-nm excitation) of Fe(III) forms of CCP(MI) and the Asn-235 and Phe-51 mutants at acid and alkaline pH (Smulevich et al., 1988a). The frequency of ν_3 is marked, from which the ligation state can be determined. The presumed interaction with a distal water molecule and with H-bonding residues is indicated in the structural diagram.

Studies of CCP mutants indicate that these factors involve interactions on both the distal and proximal side of the heme. The proximal H-bond from His-175 to Asp-235 is an important interaction since it restrains movement on the Fe toward the heme plane and also reduces the affinity for a sixth ligand electronically, by increasing the anionic character of the imidazole. When Asp-235 is replaced by Asn, the heme is completely 6-c (Smulevich et al., 1988a); a high/low-spin mixture is seen (Figure 5). Also, the pK_a for the alkaline low-spin conversion is much lower than it is for CCP(MI) (Figure 5). The H-bond from Trp-191 to Asp-235 also plays a role, since the Phe-191 mutant shows coordination behavior intermediate between those of CCP and the Asn-235 mutant (Smulevich et al., 1988). The Gly-181 mutant also shows this (Smulevich et al., 1989b), indicating a similar role for the H-bond from His-181 to the heme propionate. Both of these H-bonds provide anchor points for the His-175–Asp-235 pair.

On the distal side, W595 is H-bonded by the indole NH proton on Trp-51. It also interacts weakly with His-52 [more strongly in CCP(MI), in which His-52 is slightly closer to the heme (Wang et al., 1989)] and with another water molecule, W596, which is in turn H-bonded by Arg-48. When Trp-51 is replaced by Phe, W595 is pulled slightly farther from the Fe (Wang et al., 1989), which remains 5-c in the crystal, as confirmed by the RR spectrum of the crystal obtained with a microprobe apparatus (Smulevich et al., 1990b). In solution, however, the RR spectrum is characteristic of a mainly high-spin 6-c heme (Figure 5), implying coordination of W595. This crystal-solution difference was traced to the presence of 30% methylpentanediol in the crystallizing medium. Apparently, loss of the restraining Trp-51 H-bond allows W595 to bind to the Fe, but the amphiphilic additive reverses this tendency, perhaps by strengthening the remaining distal H-bond network. At low temperature the effect of the additive is overcome, and high-spin 6-c RR (Smulevich et al., 1990b) and EPR (Yonetani & Anni, 1987) spectra are seen.

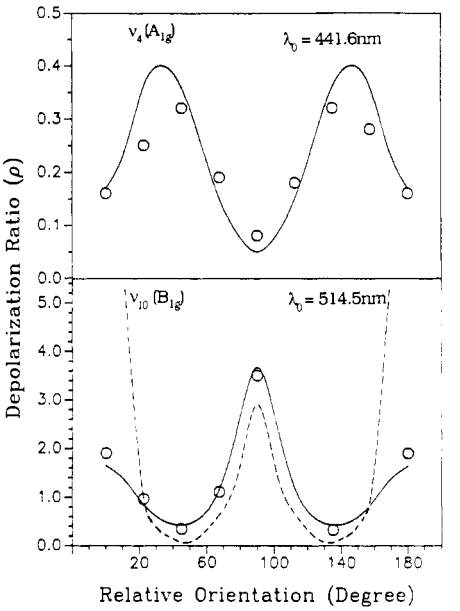

FIGURE 6: Orientation dependence of RR band depolarization ratios for single crystals of CCP mutant proteins. Experimental values (circles) for the ν_4 (A_{1g}) band (1374 cm^{-1}) of the Phe-191 mutant (top) and the ν_{10} (B_{1g}) band (1638 cm^{-1}) of the Asn-235 mutant (bottom) are compared with curves calculated on the basis of the heme orientations, assuming D_{4h} symmetry. Two directions for the x,y axes in the plane were calculated for the B_{1g} mode (the A_{1g} values are independent of the x,y directions), along the N–N directions (solid line) and rotated by 23° (dotted line). This rotation is attributed to the orienting effects of the porphyrin substituents and the protein environment. From Smulevich et al. (1990b).

At pH values below 5, a high-spin 6-c state is also seen for bakers' yeast CCP (Hashimoto et al., 1986; Smulevich et al., 1986), but this effect has been shown (Yonetani & Anni, 1987; Dasgupta et al., 1989) to result from aging of the protein to a form that is much less active than fresh protein. This form retains its high-spin character at low temperature (10 K), as does the Phe-51 mutant. In both cases the Fe–water bond must be unusually weak, because all other CCP variants show a low-spin ground state. It may be that the aging process involves a conformation change and/or irreversible modification, one of whose effect is to alter the disposition of Trp-51.

Single-crystal RR spectroscopy has also permitted the investigation of electronic effects in the heme pocket. Figure 6 shows the dependence of the depolarization ratio as a function of crystal orientation for RR bands arising from a totally symmetric mode of the Phe-191 mutant and from a nontotally symmetric mode of the Asn-235 mutant (Smulevich et al., 1990b). The data are accurately reproduced (full curves) by calculations using the crystallographically determined orientation of the heme planes and assuming 4-fold symmetry of the porphyrin. From the nontotally symmetric mode data, the electronic axes in the porphyrin plane were found empirically to be rotated by 23° relative to the lines connecting opposite pyrrole N atoms. This effect is attributed to the electronic influences of the porphyrin substituents and of the axial ligands, as well as the electrostatic field of the surrounding residues. This angle shift was different from that found for bakers' yeast CCP, 44° (Smulevich et al., 1990a), reflecting electronic changes produced by the mutation.

Fe=O Bond in the ES Complex. Reaction of CCP with H_2O_2 produces the ES complex, in which the O–O bond has been broken, leaving a Fe^{IV}=O ferryl adduct. The low-temperature crystal structure (Edwards et al., 1987) shows the Arg-48 residue moving into position to form an H-bond with the ferryl O atom, just as it does in the Fe^{III} fluoride adduct (Edwards et al., 1984). This strong H-bond probably accounts for the low Fe=O stretching frequency, 767 cm^{-1} (Hashimoto et al., 1986) or 753 cm^{-1} (Reczek et al., 1989) reported from the RR spectrum. H-Bonding is known to decrease the frequency of oxo–metal bonds substantially (Su et al., 1988). Interestingly, the frequency increases to 782 cm^{-1}, close to that observed for the analogous HRP intermediate, compound II (Hashimoto et al., 1986; Sitter et al., 1985, 1986), when the distal residue Trp-51 is replaced by Phe (J. Terner, J. R. Schifflett, J. M. Mauro, L. A. Fishel, and J. Kraut, unpublished results). In HRP the residue homologous with Trp-51 is also Phe. Thus, it appears that the Trp-51/Phe substitution disrupts the H-bond from Arg-48. For HRP compound II there is a 12-cm^{-1} downshift, 787 → 775 cm^{-1}, between high pH and neutral pH, suggesting a rather weak H-bond from the distal His residue when it is protonated. All of these frequencies are substantially lower than those observed for protein-free ferryl–heme complexes with imidazole complexes, 807–820 cm^{-1} (Schappacher et al., 1986; Kean et al., 1987), an effect attributed (Su et al., 1988) to the imidazolate character of the ligand in HRP and CCP.

Summary. Used in conjunction with site-directed mutagenesis and X-ray crystallography, RR spectroscopy can provide important information about chemical interactions at an enzyme active site. In the case of CCP, the proximal His-175–Asp-235 H-bond has been shown to be very strong by its effect on the Fe–His RR band. Indeed, the frequency and contour of this band strongly suggest that the proton in the H-bond spends about equal time on the carboxylate and imidazolate anions. RR spectroscopy can also monitor the bonding of the heme Fe with water molecules or other sixth ligands, via porphyrin marker bands of the coordination and spin state. The strong influence of the proximal H-bond is again shown by the demonstration that the substitution of Asn for Asp-235 changes the Fe(III) coordination number from 5 to 6. This is consistent with the crystallographic finding that the W595 distal water molecule moves to within bonding distance of the heme, and the RR data show, in addition, that the Fe–water bond is quite strong since the adduct is partially low spin. In contrast, a purely high-spin 6-c heme is found when Phe replaces Trp-51, but addition of an amphiphile (30% methylpentanediol) reestablishes 5-c heme, perhaps by reorganizing the distal H-bond network to facilitate the interaction of W595 with His-52 and Arg-48. Thus, in the case of the Phe-51 mutant RR spectroscopy uncovered a clear-cut difference between crystal and solution structures, which was traceable to the crystallization conditions. The technique also uncovered unusual photolability in the alkaline form of Fe(II) CCP, probably resulting from formation of a strained distal bond between the Fe and His-52 in the acid–alkaline transition. Finally, RR in conjunction with IR spectroscopy has been informative with regard to the interplay of distal and proximal interactions when CO is used as a probe molecule. The status of the Fe–N(His) bond and of the distal H-bond to the bound CO can be monitored simultaneously. The data strongly imply that the distal and proximal H-bonds are not mutually compatible and that alternative structures are formed, forms I and II, depending on which H-bond is dominant. The RR spectra indicate that a distal H-bond is not formed when CO binds to CCP(MI) but it is formed in bakers' yeast CCP when a second CO molecule binds to the protein in saturated CO solution. This difference probably results from the slightly different disposition of the His-52 side chain seen in the crystal structures. The acid–alkaline transition eliminates the distal H-bond and weakens the proximal linkage, producing a common structure for all CCP variants, form I′, whose vibrational signature is much like that of MbCO, except that the inactivity of the δ_{FeCO} mode indicates no restraint to upright binding of CO. In MbCO this mode is activated by off-axis binding, due to steric crowding by the distal His side chain. The vibrational data indicate that when the distal His is protonated in MbCO, it does not H-bond to the CO, as it does in CCP, but swings out of the pocket leaving upright CO in a hydrophobic environment. RR spectroscopy also reveals the strength of the Fe^{II}=O bond in the ES complex via the Fe–O stretching frequency and again shows large effects of both distal and proximal H-bonding.

Hemoglobin: Dynamics of Allostery

Hemoglobin is arguably the most studied of proteins. Along with myoglobin it was the first protein to have its X-ray crystal structure solved, an accomplishment for which Perutz and Kendrew won the Nobel prize in 1962. Subsequently, Monod et al. (1965) published their famous two-state theory to explain the cooperativity of ligand binding to Hb, a subject that had long excited scientific interest, and continues to do so. In this theory one state of the tetrameric protein, T (for "tense"), has a low binding affinity and is the stable form when the protein is unligated, while the other state, R (for "relaxed"), has a high binding affinity and is the stable form when the protein is ligated. The T–R switch can account for cooperative binding. The finding from crystallography that deoxyHb has one arrangement of the four subunits while ligated forms have another (Fermi & Perutz, 1981) lent plausibility to the theory and gave the two thermodynamic states a physical identification with the two quaternary structures. Subsequent research has shown this picture to be incomplete; there are more than two states available to Hb (Viggiano & Ho, 1979; Blough & Hoffman, 1984; Simolo et al., 1985; Smith & Ackers, 1985; Marden et al., 1986). But the two-state model is a very good approximation under normal conditions of ligand binding to native Hb (Shulman et al., 1975), and there is little question that the T–R switch is the central event in the regulation of ligand binding.

The mechanism of this switch is the most interesting question about Hb from a molecular point of view. How is a large-scale rearrangement of the subunits initiated by the simple act of binding ligands to the heme groups? The most fruitful approach to this question is to elucidate the kinetic steps in the R–T transition consequent to photodissociation of heme-bound ligands. Following absorption of a photon by the heme group, the axial ligands dissociate efficiently and in most cases recombine on the picosecond time scale (Jongeward et al., 1988); CO however recombines slowly enough that most of it escapes from the protein (Hofrichter et al., 1983). A deoxy heme absorption spectrum develops immediately (0.35 ps) after photolysis (Martin et al., 1983) and remains essentially unchanged out to nanoseconds (Greene et al., 1978; Sawicki & Gibson, 1976). Small changes in this spectrum have been detected on a longer time scale, yielding relaxation times of ~0.1, ~1, and ~20 μs (Hofrichter et al., 1983). These changes no doubt reflect the influence of protein rearrangements on the heme electronic structure. The 20-μs process coincides with the transition between fast and slow second-order CO binding processes discovered by Gibson and

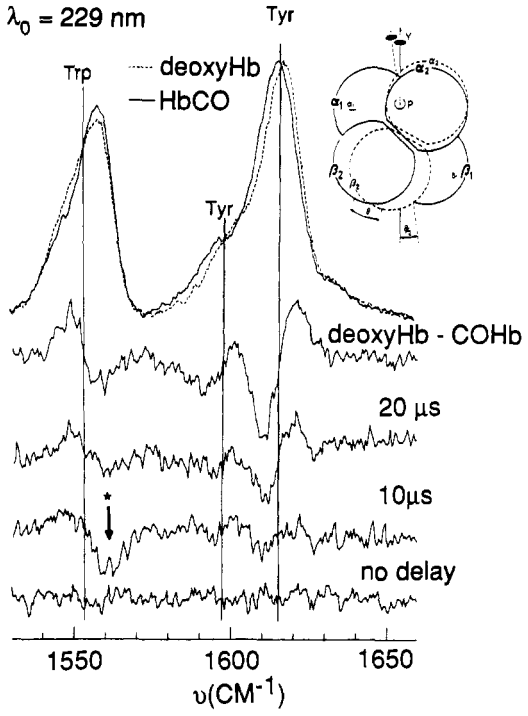

FIGURE 7: UVRR spectra of HbCO and deoxyHb (top) and their difference, compared with difference spectra of the HbCO photoproduct generated with a 532-nm photolysis pulse at the indicated delay prior to a 239-nm probe pulse. The difference signals are attributed to the Tyr-α_{42} and Trp-β_{37} residues at the $\alpha_1\beta_2$ interface, whose H-bonding is altered via the subunit rearrangement (inset) in the R–T transition. From Su et al. (1989).

co-workers (Gibson, 1959; Sawicki & Gibson, 1976) and attributed to the R–T quaternary rearrangement. The earlier processes are then plausibly attributed to tertiary changes on the pathway to the R–T switch. Transient RR spectroscopy has provided insight into the nature of these processes.

Aromatic Residue Changes Monitor the R–T Transition. When the RR spectrum with UV excitation at 229 nm is measured carefully, small shifts are seen between HbO_2 or HbCO, which give identical spectra, and deoxyHb (Su et al., 1989) (Figure 7). The difference spectrum clearly shows a downshift in the 1555-cm^{-1} band, arising from tryptophan residues, and upshifts in the 1615-cm^{-1} band and its 1600-cm^{-1} shoulder, arising from tyrosine residues (Rava & Spiro, 1985). When the UV excitation pulses are overlapped with 532-nm photolyzing pulses in a flowing solution of HbCO, the difference spectrum, relative to unphotolyzed HbCO, is featureless and remains so when the probe pulses are delayed by up to 1 μs (Su et al., 1989). Difference bands begin to appear at 5 μs, and at a 20-μs delay one sees a difference spectrum that closely resembles the static deoxyHb – HbCO difference spectrum (Figure 7). Thus, the aromatic residues are sensing a process with the same timing as the last optical transient of the deoxy heme group, and the transition from fast to slow CO rebinding rates. The perturbation of the aromatic groups is the same as that shown between Hb in the T vs the R quaternary structure.

The Hb tetramer has three inequivalent Trp and six inequivalent Tyr residues, occurring in equivalent pairs. Most of these do not show significant changes in their environments when the HbCO and deoxyHb crystal structures are compared (Fermi & Perutz, 1981). Two of the residues, however, Trp-β_{37} and Tyr-α_{42}, are at the $\alpha_1\beta_2$ subunit interface, where most of the displacements occur between the R and T structures (Baldwin & Chothea, 1979). The indole NH proton of Trp-β_{37} is H-bonded to the backbone carbonyl of Asn-β_{102} in the R state but to the carboxylate side chain of Asp-α_{94} in the T state. The Tyr-α_{42} OH group accepts an H-bond from the peptide NH of Asp-α_{94} in both states, but in the T state it also forms a donor interaction with the side chain of Asp-β_{99}. The UVRR band shifts are plausibly attributed to these H-bonding changes. Thus, the transient UVRR difference spectra provide direct structural evidence that the 20-μs transition is the R–T subunit rearrangement.

Fe–His Stretch Evolves over Several Time Scales. Although the proximal His side-chain is H-bonded to a backbone carbonyl group in both Mb and Hb (Fermi & Perutz, 1981; Baldwin & Chothea, 1979), the Fe–His stretching frequency is at a distinctly lower frequency, 215 vs 220 cm^{-1}, in Hb (Kincaid et al., 1979; Nagai et al., 1980) than in Mb (Kitagawa et al., 1979; Argade et al., 1984). When, however, chemically modified or mutant Hb's are examined, in which the quaternary constraints are relaxed and the R state is stable even in the deoxy form, then the Fe–His frequency is 222 cm^{-1} (Nagai et al., 1980), near that in Mb. Likewise, a 223-cm^{-1} frequency was observed when the R state was isolated kinetically, by photolyzing HbCO in a flowing stream of sample, with a 0.3-μs residence time in the laser beam (Stein et al., 1982), shorter than the R–T relaxation time. Thus the Fe–His frequency decreases in the T state and is linked to the quaternary structure. Since a decreased frequency implies a weakened bond, the RR data provide a definite indication that there really is molecular tension in the T state (Perutz, 1975).

The molecular mechanism responsible for the bond weakening is not entirely clear, however. Weakened H-bonding to the backbone carbonyl group has been considered (Stein et al., 1980), but the behavior of the imidazole proton NMR resonances seems to argue against this interpretation (La Mar & De Ropp, 1982). Alternatively, tilting of the imidazole ring relative to the heme normal, as seen in the deoxyHb crystal structure (Baldwin & Chothea, 1979), has been suggested to weaken the Fe–His bond due to the resulting nonbonded repulsion between the imidazole and the pyrrole ring toward which it bends (Gelin & Karplus, 1977; Friedman et al., 1982; Scott & Friedman, 1984). The observed tilt is greater in Mb [11° (Takano, 1977)] than in Hb [7° (Baldwin & Chothea, 1979)], however, and Fermi et al. (1984) have questioned whether the nonbonded contact is significant in the deoxyHb structure. It has also been argued that rotation of the imidazole relative to the Fe–pyrrole bonds, together with the tilt, can modulate the Fe–His bonding via a repulsive interaction between the Fe d_{z^2} and the porphyrin π orbitals (Bangcharoenparpong et al., 1984). Finally, it cannot be ruled out that a straightforward mechanical force stretches the Fe–His bond, inasmuch as the F-helix, which contains the proximal His residue, is displaced by about 1 Å relative to the heme plane in the R–T transition (Baldwin & Chothea, 1979). Any or all of these factors could, of course, operate simultaneously. Interestingly, the T-state Fe–His frequency shift is much greater for the α than for the β chains, in line with Pertuz' view that the lowering of ligand affinity in the T state is due to proximal constraints in the α chains but to steric hindrance on the distal side in the β chains (Perutz, 1975). Using chain-specific valency hybrids, Nagai and Kitagawa (1980) showed that the R- and T-state frequencies were 222 and 218 cm^{-1} for the β chains but 220 and 205 cm^{-1} for the α chains. Similar results were obtained with Co,Fe hybrids (Ondrias et al., 1982).

While the Fe–His frequency is higher in the R than in the T state, Friedman and co-workers have shown that it is still higher, 230 cm^{-1}, in the HbCO photoproduct generated with

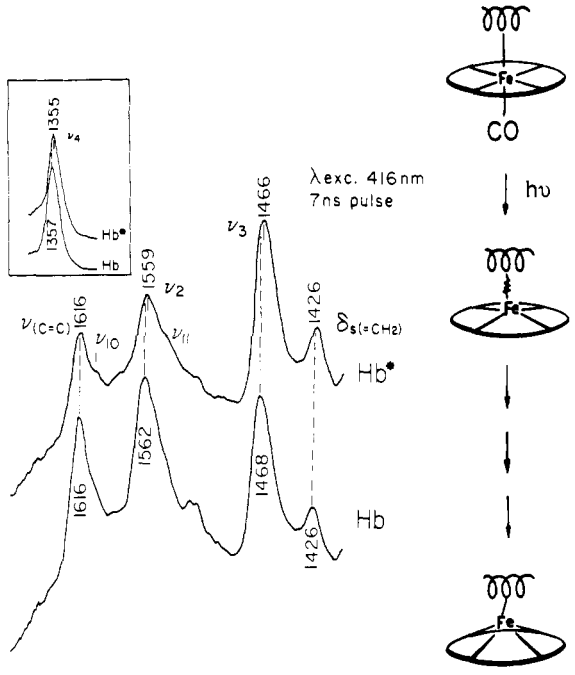

FIGURE 8: RR spectra in the 1400–1650-cm^{-1} core-size marker band region for the HbCO photoproduct (Hb*) generated with 7-ns 416-nm pulses, showing 2–3-cm^{-1} downshifts relative to deoxyHb, of ν_2 and ν_3 and also of ν_4 (inset). The $\nu_{C=C}$ and $\delta_{2(=CH_2)}$ vinyl modes are unshifted, however. Schematic structures illustrate the proposed restraint on the Fe out-of-plane motion by the F-helix in Hb*. Adapted from Dasgupta and Spiro (1986).

10-ns (Friedman et al., 1982) or 25-ps (Findsen et al., 1985) laser pulses. Thus the frequency is elevated immediately after photolysis and remains constant for the first few nanoseconds. It evolves toward the R-state frequency on a time scale of about a microsecond, as shown by pulse–probe experiments (Scott & Friedman, 1984). Thus, during the ~1-μs tertiary transient seen in the absorption kinetics, the Fe–His bond relaxes to its R-state character. This behavior has been discussed extensively in terms of the evolution of the imidazole from an upright orientation in HbCO to a tilted one in deoxyHb (Scott & Friedman, 1984). But it seems likely that the frequency elevation immediately after photolysis is at least partly due to protein restraint on the out-of-plane displacement of the Fe atom, as discussed in the next section.

Early Restraint on the Fe Out-of-Plane Displacement. When the porphyrin RR bands of the HbCO photoproduct were examined with 30-ps (Terner et al., 1981) or 7-ns (Dasgupta & Spiro, 1986) laser pulses, the core-size marker band frequencies were found to be 2–3 cm^{-1} lower than those in deoxyHb. As shown in Figure 8, these differences do not arise from a generalized spectral shift, since no shift is seen for the vinyl modes at 1616 and 1426 cm^{-1} but only for the core-size markers ν_2 and ν_3 at 1562 and 1468 cm^{-1} [also ν_{10}, ν_{11}, and ν_{19}, which are brought out with 532-nm excitation (Dasgupta & Spiro, 1986)]. These results imply that the core size is slightly larger than that in the final deoxyHb. If as is generally accepted photolysis occurs via intersystem crossing to a high-spin state of the 6-c heme-CO adduct (Greene et al., 1978; Waleh & Lowe, 1982), then the porphyrin core must initially be substantially expanded. But it relaxes to a somewhat smaller value as the Fe moves out of the plane in the 5-c deoxy heme. The Fe motion may, however, be constrained by protein forces, and full relaxation of the core size can thereby be coupled to protein motions. Detailed consideration of the geometry and RR frequencies of 5-c and 6-c high-spin Fe(II) hemes led to the estimate that the restraint on the out-of-plane displacement in the prompt photoproduct is about 0.1 Å out of the 0.4-Å displacement in deoxyHb (Dasgupta & Spiro, 1986). Dynamics calculations (Henry et al., 1985) indicate very rapid (50–150 fs) motion of the Fe atom out of the plane, due to nonbonded imidazole–pyrrole forces which are uncompensated when the Fe–CO bond breaks (Friedman et al., 1982), but the amplitude of the motion was slightly smaller when the protein was included in the calculation, consistent with the proposed 0.1-Å pause.

The core-size frequencies are fully relaxed to the deoxyHb values when examined within 0.3 μs (Stein et al., 1982), suggesting that the 0.1-μs optical transient is associated with a protein motion allowing full out-of-plane displacement of the Fe. Interestingly, the marker bands of the MbCO photoproduct are also downshifted relative to those of deoxyMb when examined with 30-ps pulses but are fully relaxed when examined with 7-ns pulses; preliminary data suggest a 0.2-ns relaxation time (Dasgupta et al., 1985). Thus, the protein motion reponsible for the core-size relaxation is about 3 orders of magnitude faster for Mb than for Hb. This motion may be associated with the proximal F-helix, which is displaced by 1.0 Å relative to the heme group in deoxyHb vs ligated Hb (Baldwin & Chothea, 1979) but by only 0.1 Å in deoxyMb vs ligated Mb (Baldwin & Chothea, 1979).

If protein forces restrain the Fe out-of-plane displacement, then the Fe–His bond might be compressed at early times, perhaps accounting for at least part of the elevation of the Fe–His frequency in the prompt HbCO photoproduct. Part of the relaxation of this frequency does occur in the first 0.4 μs (Scott & Friedman, 1984), but part of it continues into the microsecond regime, after the core size has relaxed completely. Thus, the first protein motion (0.1 μs) allows full Fe displacement, while further relaxation of the Fe–His bond continues with the second protein motion (1 μs).

Mystery of ν_4. The porphyrin skeletal mode ν_4, a breathing vibration at ~1360 cm^{-1} which involves the pyrrole C–N bonds primarily (Li & Spiro, 1988a), gives rise to the strongest band in heme protein RR spectra when in resonance with the dominant Soret electronic transition near 400 nm. It has been studied extensively, but interpretation is somewhat clouded by its apparent sensitivity to multiple stereoelectronic factors. Thus, its frequency is only weakly sensitive to the core size (Parthasarathi et al., 1987) but strongly dependent on the occupancy of the porphyrin HOMO and LUMO, as seen in the spectra of radical cation (Czernuszewicz et al., 1989) and anion (Atamain et al., 1989) species, and therefore sensitive to the electronic effects of back-bonding (Spiro & Burke, 1976). It is also sensitive to the Fe oxidation state (Spiro & Strekas, 1974; Yamamoto et al., 1973), although this may be a fortuitous result of separate deviations from the frequencies expected on the basis of core size for low- and high-spin Fe(II), the former due to back-bonding and the latter due to doming of the porphyrin ring (Parthasarathi et al., 1987).

Like the core-size markers, ν_4 is 2 cm^{-1} lower in the HbCO photoproduct monitored with 7-ns laser pulses than it is in deoxyHb, but it does not relax within 0.3 μs, as the core size sensitive ν_2 does (Stein et al., 1982). Rather, the ν_4 downshift appears to relax in concert with the 1- and 20-μs optical transients (Friedman & Lyons, 1980), just as the Fe–His frequency does. Indeed, the Fe–His frequency correlates accurately with ν_4 for a variety of deoxyHb's, in both R and T states (Rousseau & Ondrias, 1983). Thus within the molecular architecture of Hb (the correlation does not extend to other heme proteins, such as the peroxidases), the factors that determine the Fe–His frequency also determine the ν_4 fre-

quency. Whether this effect is due to the electron density on the Fe atom, as modulated by the strength of the Fe–His bond, or to some correlated parameter of the porphyrin ring, e.g., doming, is uncertain.

Recently, Petrich et al. (1987) have set a timing record for transient RR spectroscopy by monitoring ν_4 of the HbCO photoproduct with 0.2-ps pump and probe pulses. Although the pump pulse had a large frequency width, 35 cm^{-1}, they deconvoluted the RR band from the instrument response to obtain 2–11-cm^{-1} frequency differences relative to deoxyHb. The largest difference was seen at the earliest delay, 0.9 ps. The difference quickly fell to 2 cm^{-1}, at a 10-ps delay, and then rose again to 4 cm^{-1} at 95 ps. The authors attributed the first phase to vibrational cooling of the temperature rise associated with the excess energy of the photolysis pulse and the second phase to a structural relaxation, perhaps associated with the Fe–His bond. Dynamical calculations do indicate that local heating from the photolysis pulse is significant on the scale of 10 ps (Henry et al., 1985), but it is not clear that an 11-cm^{-1} shift can be produced by this effect since ν_4 is known to vary only 3 cm^{-1} in deoxyHb between 4 and 300 K (Rousseau & Friedman, 1988); the temperature dependence of the ν_{10} band of NiOEP (Asher & Murtaugh, 1983), which was used to rationalize the result, is not an appropriate reference, since it stems from porphyrin ruffling dynamics, which are specific to the Ni porphyrin (Czernuszewicz et al., 1989b). It is also hard to understand how the frequency upshift between 10 and 95 ps could be caused by Fe–His bond relaxation. The Fe–His frequency itself shows no change between 25 ps and 7 ns (Findsen et al., 1985). Thus, these intriguing results suggest the need for further experiments with very short pulses, monitoring other modes besides ν_4, including, if possible, the Fe–His mode itself.

Summary. Because vibrational frequencies are sensitive to structure, RR spectroscopy can provide structural information about kinetic steps in protein transformations when carried out in a time-resolved mode. UVRR spectroscopy has shown that the aromatic groups of the HbCO photoproduct respond with a delay of 20 μs and has provided direct structural evidence that the 20-μs kinetic step is the R–T quaternary rearrangement of the subunits. RR bands of the porphyrin ring show that the core relaxes via a 0.1-μs protein motion, which probably allows the Fe atom to attain its full out-of plane displacement. The Fe–His stretching frequency has an elevated value immediately after CO photolysis, in part, perhaps, because of the protein constraint on the Fe displacement. It relaxes on both the 0.1- and 1-μs time scales to its value in R-state Hb and then decreases further to its T-state value. These changes may be connected with reorientation of the proximal His side chain. At very early times after a photolysis pulse, heating effects may be an important aspect of the protein dynamics, but further experiments are needed to understand the RR response.

Registry No. CCP, 9029-53-2.

References

Argade, P. V., Sassaroli, M., Rousseau, D. L., Inubushi, T., Ikeda-Saito, M., & Lapidot, A. (1984) *J. Am. Chem. Soc. 106*, 6593–6596.

Asher, S. A., & Murtaugh, J. (1983) *J. Am. Chem. Soc. 105*, 7244–7251.

Asher, S. A., Johnson, C. R., & Murtaugh, J. (1983) *Rev. Sci. Instrum. 54*, 1657.

Atamain, M., Donahoe, R. J., Lindsay, J. S., & Bocian, D. F. (1989) *J. Phys. Chem. 93*, 2236.

Baldwin, J. M., & Chothea, C. J. (1979) *J. Mol. Biol. 129*, 175–201.

Bancharoenpaurpong, O., Shoemacker, K. T., & Champion, P. M. (1984) *J. Am. Chem. Soc. 106*, 5688.

Beinert, H., & Thomson, A. J. (1983) *Arch. Biochem. Biophys. 222*, 333.

Blough, N. V., & Hoffman, B. M. (1984) *Biochemistry 23*, 2875–2882.

Carey, P. R. (1988) in *Biological Applications of Raman Spectroscopy* (Spiro, T. G., Ed.) Vol. 2, Chapter 6, Wiley, New York.

Cassatt, J. C., Marini, C. P., & Bender, J. (1975) *Biochemistry 14*, 5470.

Champion, P. M. (1988) in *Biological Applications of Raman Spectroscopy* (Spiro, T. G., Ed.) Vol. 3, pp 249–992, Wiley, New York.

Chen, D., Yue, K.-T., Martin, C., Rhee, K. W., Sloan, D., & Callender, R. (1987) *Biochemistry 26*, 4776.

Chernoff, D. A., Hochstrasser, R. M., & Steele, A. W. (1980) *Proc. Natl. Acad. Sci. U.S.A. 77*, 5606.

Collman, J. P., & Reed, C. A. (1973) *J. Am. Chem. Soc. 95*, 2068.

Czernuszewicz, R. S., Macor, K. A., Kincaid, J. R., & Spiro, T. G. (1989a) *J. Am. Chem. Soc. 111*, 3860.

Czernuszewicz, R. S., Li, X.-Y., & Spiro, T. G. (1989b) *J. Am. Chem. Soc. 111*, 7024–7031.

Dasgupta, S., & Spiro, T. G. (1986) *Biochemistry 25*, 5941–5948.

Dasgupta, S., Spiro, T. G., Johnson, C. K., Delickas, G. A., & Hochstrasser, R. M. (1985) *Biochemistry 24*, 5295–5297.

Dasgupta, S., Rousseau, D., Anni, H., & Yonetani, T. (1989) *J. Biol. Chem. 264*, 654.

Derguini, F., Dunn, D., Eisenstein, L., Nakanishi, K., Odashima, K., Rao, V. J., Sastry, L., & Termini, J. (1986) *Pure Appl. Chem. 58*, 719.

Edwards, S. L., & Poulos, T. L. (1990) *J. Biol. Chem. 265*, 2588.

Edwards, S. L., Poulos, T. L., & Kraut, J. (1984) *J. Biol. Chem. 259*, 12984.

Edwards, S. L., Yuong, Ng. H., Hamlin, R. C., & Kraut, J. (1987) *Biochemistry 26*, 1503.

Evangelista-Kirkup, R., Smulevich, G., & Spiro, T. G. (1986) *Biochemistry 25*, 4420.

Fermi, G., & Perutz, M. F. (1981) *Atlas of Molecular Structures in Biology, to Hemoglobin and Myoglobin*, Clarendon Press, Oxford.

Fermi, G., Perutz, M. F., Shanan, B., & Foerm, R. (1984) *J. Mol. Biol. 175*, 159.

Findsen, W., Friedman, J. M., Ondrias, M. R., & Simon, S. R. (1985) *Science 229*, 661–665.

Finzel, B. C., Poulos, T. L., & Kraut, J. (1984) *J. Biol. Chem. 259*, 13027.

Fodor, S. P. A., Rava, R. P., Copeland, R. A., & Spiro, T. G. (1986) *J. Raman Spectrosc. 17*, 471.

Friedman, J. M., & Lyons, K. B. (1980) *Nature 284*, 570.

Friedman, J. M., Rousseau, D. L., Ondrias, M. R., & Stepnoski, R. A. (1982) *Science 218*, 1244.

Gelin, B. R., & Karplus, M. (1977) *Proc. Natl. Acad. Sci. U.S.A. 74*, 801.

George, S. J., Richards, A. J. M., Thomson, A. J., & Yates, M. G. (1984) *Biochem. J. 224*, 247.

Ghosh, D., O'Donnell, S., Furey, W., Jr., Robbins, A. H., & Stout, C. D. (1982) *J. Mol. Biol. 158*, 73.

Gibson, Q. H. (1959) *Biochem. J. 71*, 293–303.

Goodin, D. B., Mauk, A. G., & Smith, H. (1986) *Proc. Natl. Acad. Sci. U.S.A. 83*, 1295.

Greene, B. I., Hochstrasser, R. M., Weisman, R. B., & Eaton, W. A. (1978) *Proc. Natl. Acad. Sci. U.S.A. 75*, 5255.

Hashimoto, S., Tatsuno, Y., & Kitagawa, T. (1986) *Proc. Natl. Acad. Sci. U.S.A. 83*, 2417.

Henry, E. R., Levitt, M., & Eaton, W. A. (1985) *Proc. Natl. Acad. Sci. U.S.A. 82*, 2034–2038.

Hofrichter, J., Sommer, J. H., Henry, E. R., & Eaton, W. A. (1983) *Proc. Natl. Acad. Sci. U.S.A. 80*, 2235.

Hudson, B. S., & Mayne, L. C. (1988) in *Biological Applications of Raman Spectroscopy* (Spiro, T. G., Ed.) Vol. 2, Chapter 4, Wiley, New York.

Iizuka, T., Makino, R., Ishimura, Y., & Yonetani, T. (1985) *J. Biol. Chem. 260*, 1407.

Jogenward, K. A., Magde, D., Taube, D. J., & Traylor, T. G. (1988) *J. Biol. Chem. 263*, 6027.

Johnson, M. K., Czernuszewicz, R. S., Spiro, T. G., Fee, J. A., & Sweeney, W. V. (1983) *J. Am. Chem. Soc. 105*, 6671.

Jones, C. M., Devito, V. L., Harmon, P. A., & Asher, S. A. (1987) *Appl. Spectrosc. 41*, 1268.

Jongeward, K. A., Magde, D., Taube, D. J., & Traylor, T. G. (1988) *J. Biol. Chem. 263*, 6027.

Kean, R. T., Oertling, W. A., & Babcock, G. T. (1987) *J. Am. Chem. Soc. 109*, 2185–2187.

Kerr, E. R., & Yu, N.-T. (1988) in *Biological Applications of Raman Spectroscopy* (Spiro, T. G., Ed.) Vol. 3, pp 39–96, Wiley, New York.

Kim, K., Fettinger, J., Sessler, J. L., Cyr, M., Hugdahl, J., Collman, J. P., & Ibers, J. A. (1989) *J. Am. Chem. Soc. 111*, 403.

Kincaid, J., Stein, P., & Spiro, T. G. (1979) *Proc. Natl. Acad. Sci. U.S.A. 76*, 4156.

Kitagawa, T. (1988) in *Biological Applications of Raman Spectroscopy* (Spiro, T. G., Ed.) Vol. 3, pp 97–132, Wiley, New York.

Kitagawa, T., Nagai, K., & Tsubaki, M. (1979) *FEBS Lett. 104*, 376.

Kuriyan, J., Wilz, S., Karplus, M., & Petsko, G. A. (1986) *J. Mol. Biol. 192*, 133.

La Mar, G. N., & de Ropp, J. S. (1979) *Biochem. Biophys. Res. Commun. 90*, 36.

La Mar, G. N., & de Ropp, J. S. (1982) *J. Am. Chem. Soc. 104*, 5203–5206.

Li, X.-Y., & Spiro, T. G. (1988a) in *Biological Applications of Raman Spectroscopy* (Spiro, T. G., Ed.) Vol. 3, Chapter 1, Wiley, New York.

Li, X.-Y., & Spiro, T. G. (1988b) *J. Am. Chem. Soc. 105*, 7781.

Marden, M. C., Hazard, E. S., & Gibson, Q. H. (1986) *Biochemistry 25*, 7591–7596.

Martin, J. L., Migus, A., Poyart, C., LeCarpentier, T., Astier, R., & Antosetti, A. (1983) *Proc. Natl. Acad. Sci. U.S.A. 80*, 173.

Mauro, J. M., Miller, M. A., Edwards, S. L., Wang, J., Fishel, L. A., & Kraut, J. (1989) *Met. Ions Biol. Syst. 25*, 477–503.

Miller, M. A., Coletta, M., Mauro, J. M., Putnam, L. D., Farnum, M. F., Kraut, J., & Traylor, T. G. (1990) *Biochemistry 29*, 1777.

Monod, J., Wyman, J., & Changeux, J. P. (1965) *J. Mol. Biol. 12*, 88.

Nagai, K., & Kitagawa, T. (1980) *Proc. Natl. Acad. Sci. U.S.A. 77*, 2033–2037.

Nagai, K., Kitagawa, T., & Morimoto, H. (1980) *J. Mol. Biol. 136*, 271–289.

Ondrias, M. R., Rousseau, D. L., Kitagawa, T., Ikeda-Saito, M., Inobushi, T., & Yonetani, T. (1982) *J. Biol. Chem. 257*, 8766–8770.

Parthasarathi, N., Hansen, C., Yamaguchi, S., & Spiro, T. G. (1987) *J. Am. Chem. Soc. 109*, 3865.

Perutz, M. F. (1975) *Br. Med. Bull. 32*, 195–207.

Perutz, M. F., Fermi, G., Luisi, B., Shaanan, B., & Liddington, R. C. (1987) *Acc. Chem. Res. 20*, 309.

Petrich, J. W., Martin, J. L., Houda, D., Poyart, C., & Orszag, A. (1987) *Biochemistry 26*, 7914–7923.

Poulos, T. L. (1988) *Adv. Inorg. Biochem. 7*, 1–36.

Poulos, T. L., & Kraut, J. (1980) *J. Biol. Chem. 255*, 8199.

Ramsden, J., & Spiro, T. G. (1989) *Biochemistry 28*, 3125.

Rava, R. P., & Spiro, T. G. (1985) *J. Phys. Chem. 89*, 1856.

Ray, G., Li, X.-Y., Sessler, J. L., & Spiro, T. G. (1989) (in preparation).

Reczek, C. M., Sitter, A. J., & Terner, J. (1989) *J. Mol. Struct.* (in press).

Rousseau, D. L., & Ondrias, M. R. (1983) *Annu. Rev. Biophys. Bioeng. 12*, 357–380.

Rousseau, D. L., & Friedman, J. M. (1988) in *Biological Applications of Raman Spectroscopy* (Spiro, T. G., Ed.) Vol. 3, pp 172–180, Wiley, New York.

Satterlee, I. D., & Erman, J. E. (1984) *J. Am. Chem. Soc, 106*, 1139.

Sawicki, C., & Gibson, Q. H. (1976) *J. Biol. Chem. 251*, 1533.

Schappacher, M., Chottard, G., & Weiss, R. (1986) *J. Chem. Soc., Chem. Commun.*, 93–94.

Scott, T. W., & Friedman, J. M. (1984) *J. Am. Chem. Soc. 106*, 5677.

Shulman, R. G., Hopfield, J. J., & Ogawa, S. (1975) *Q. Rev. Biophys. 8*, 325–420.

Simolo, K., Stucky, G., Chen, S., Bailey, M., Scholes, C., & McLendon, G. (1985) *J. Am. Chem. Soc. 107*, 2865–2872.

Sitter, A. J., Shiffett, J. R., & Terner, J. (1988) *International Conference on Raman Spectroscopy* (Clark, R. J. H., & Long, D. A., Eds.) pp 659–660, Wiley, London.

Sivaraja, M., Goodin, D. B., Mauk, A. G., Smith, M., & Hoffman, B. M. (1989) *Science 245*, 738.

Smith, F. R., & Ackers, G. K. (1985) *Proc. Natl. Acad. Sci. U.S.A. 82*, 5347–5351.

Smith, M. L., Ohlsson, P.-J., & Paul, K. G. (1983) *FEBS Lett. 163*, 303.

Smulevich, G., Evangelista-Kirkup, R., English, A. M., & Spiro, T. G. (1986) *Biochemistry 25*, 4426.

Smulevich, G., Mauro, J. M., Fishel, L. A., English, A. M., Kraut, J., & Spiro, T. G. (1988a) *Biochemistry 27*, 5477.

Smulevich, G., Mauro, J. M., Fishel, L. A., English, A. M. Kraut, J., & Spiro, T. G. (1988b) *Biochemistry 27*, 5486.

Smulevich, G., Mantini, A. R., English, A. M., & Mauro, J. M. (1989a) *Biochemistry 28*, 5058.

Smulevich, G., Miller, M. A., & Spiro, T. G. (1989b) (in preparation).

Smulevich, G., Miller, M. A., Gosztola, D., & Spiro, T. G. (1989c) *Biochemistry 28*, 9905.

Smulevich, G., Wang, Y., Edwards, S. L., Poulos, T. L., English, A. M., & Spiro, T. G. (1990a) *Biochemistry 29*, 2586.

Smulevich, G., Wang, Y., Mauro, J. M., Wang, J., Fishel, L. A., Kraut, J., & Spiro, T. G. (1990b) *Biochemistry* (in press).

Spiro, T. G., Ed. (1988) *Biological Applications of Raman Spectroscopy*, Vols. 1–3, Wiley, New York.

Spiro, T. G., & Strekas, T. C. (1974) *J. Am. Chem. Soc. 96*, 338.

Spiro, T. G., & Burke, J. M. (1976) *J. Am. Chem. Soc. 98*, 5482–5489.

Spiro, T. G., & Stein, P. (1977) *Annu. Rev. Phys. Chem. 28*, 501.

Spiro, T. G., & Li, X.-Y. (1988) in *Biological Applications of Raman Spectroscopy* (Spiro, T. G., Ed.) Vol. 3, pp 1–38, Wiley, New York.

Stein, P., Mitchell, M., & Spiro, T. G. (1980) *J. Am. Chem. Soc. 102*, 7795.

Stein, P., Terner, J., & Spiro, T. G. (1982) *J. Phys. Chem. 86*, 168–170.

Stout, C. D. (1988) *J. Biol. Chem. 263*, 9256.

Stout, G. H., Turley, S., Sieker, L. C., & Jensen, L. H. (1988) *Proc. Natl. Acad. Sci. U.S.A. 85*, 1020.

Su, C., Park, Y. D., Liu, G.-Y., & Spiro, T. G. (1989) *J. Am. Chem. Soc. 111*, 3457.

Takano, T. (1977) *J. Mol. Biol. 110*, 569–584.

Teraoka, J., & Kitagawa, T. (1981) *J. Biol. Chem. 256*, 3969.

Teraoka, J., Job, D., Morita, Y., & Kitagawa, T. (1983) *Biochim. Biophys. Acta 747*, 10.

Terner, J., Stong, J. D., Spiro, T. G., Nagumo, M., Nicol, M. S., & El-Sayed, M. A. (1981) *Proc. Natl. Acad. Sci. U.S.A. 78*, 1313–1317.

Terner, J., Schifflett, J. R., Mauro, J. M., Fishel, L. A., & Kraut, J. (1989) (in preparation).

Tsubaki, M., Srivastava, R. B., & Yu, N.-T. (1982) *Biochemistry 21*, 1132.

Tsuboi, M., Nishimura, Y., Hirakawa, A. Y., & Peticolas, W. (1988) in *Biological Applications of Raman Spectroscopy* (Spiro, T. G., Ed.) Vol. 2, Chapter 3, Wiley, New York.

Uno, T., Nishimura, Y., Tsuboi, M., Makino, R., Iizuka, T., & Ishimura, Y. (1987) *J. Biol. Chem. 262*, 4549.

Viggiano, G., & Ho, C. (1979) *Proc. Natl. Acad. Sci. U.S.A. 76*, 3673–3677.

Waleh, A., & Lowe, G. H. (1982) *J. Am. Chem. Soc. 104*, 2346.

Wang, J., Mauro, M. J., Fishel, L. A., Edwards, S. L., Oatley, S. J., Yuong, Ng. H., & Kraut, J. (1989) *Biochemistry* (submitted for publication).

Yamamoto, T., Palmer, G., Gill, D., Salmeen, I. T., & Remi, L. (1973) *J. Biol. Chem. 248*, 5211.

Yonetani, T. (1976) *Enzymes (3rd Ed.) 13*, 345.

Yonetani, T., & Anni, H. (1987) *J. Biol. Chem. 262*, 9547.

Yu, N.-T., Kerr, E. A., Ward, B., & Chang, C. K. (1983) *Biochemistry 22*, 4534.

Ziegler, L. D., & Hudson, B. S. (1983) *J. Chem. Phys. 79*, 1139.